Colloid Polym Sci (2005) 284: 340–345
DOI 10.1007/s00396-005-1385-3

SHORT COMMUNICATION

Jinping Dong
Guangzhao Mao

Polystyrene nanorod formation in $C_{12}E_5$ hemimicelle thin film templates

Received: 9 June 2005
Accepted: 20 July 2005
Published online: 30 September 2005

J. Dong · G. Mao (✉)
Department of Chemical Engineering
and Materials Science,
Wayne State University, Detroit,
MI 48202, USA
E-mail: gzmao@eng.wayne.edu

J. Dong
University of Minnesota,
350 Shepherd Laboratories,
100 Union St., SE, Minneapolis,
MN 55455, USA

Abstract This paper reports the synthesis and characterization of polystyrene nanorods in hemicylindrical hemimicelles of a nonionic polyoxyethylene surfactant, $C_{12}E_5$, on graphite. The surface structure is characterized by atomic force microscopy (AFM), Fourier transform infrared spectroscopy, and contact angle goniometry. Uniformly aligned polystyrene nanorods are captured by AFM. The nanorod dimensions are studied as a function of the reaction time and styrene monomer concentration. The template synthesis using self-assembled surfactant surface aggregates promises to create functional and stable nanostructures for optoelectronics and surface engineering.

Keywords Aggregation · Micelles · Nanostructures · Surfactants · Template Synthesis

Introduction

Surfactants self-associate into micelles with various radii of curvature, vesicles, and ordered liquid crystalline phases at the concentration above the critical micelle concentration (CMC) [1]. Recent atomic force microscopy (AFM) studies have shown that analogous structural transitions also occur at the solid/liquid interface. At the solid/liquid interface, surfactants self-assemble into discrete surface micelles with spherical, cylindrical, and disk-like shapes, in addition to the normal continuous monolayer and bilayer structures [2–7]. Previously, surfactant micelles, reversed micelles, micro-emulsions, vesicles, tubules, and liquid crystalline phases have been used as templates for nanostructured material synthesis with retention of the original template microstructure [8, 9]. The self-assembled structures of surfactants at surfaces may also serve as templates for the synthesis of nanostructured thin films by following similar recipes used in bulk mesophase synthesis. The nanostructured thin films may have applications in ultrafine separations, optoelectronic arrays, and surface modification.

Polymerization in surfactant mesophases follows two synthesis routes. One uses the polymerizable surfactants [10] and the other relies on the localized solubilization of monomers in surfactant mesophases [11]. The two strategies can be combined to synthesize copolymers by

reacting polymerizable surfactants with localized monomers. The same strategies have been adopted to synthesize textured polymer films using the self-assembled structures of surfactants at surfaces, sometimes referred to as admicelle polymerization [12]. Monomers, such as styrene, isoprene, pyrrole, and butadiene, have been polymerized in the hydrophobic interior of admicelles on a variety of surfaces including silica particles, alumina, mica, glass fibers, and cotton fibers. The highly oriented pyrolytic graphite (HOPG) has been a popular choice because alkyl surfactants self-assemble into highly ordered hemicylindrical hemimicelles as a result of one-dimensional (1-D) epitaxy. Polymeric nanorod arrays have been synthesized from polymerizable surfactant surface micelles on mica [13] and monomers dispersed in surfactant surface micelles on HOPG [14, 15]. Here we report the synthesis of polymeric nanorod arrays from a common monomer, styrene, within a nonionic polyoxyethylene surfactant hemimicelle template on HOPG.

Results and discussions

The surfactant hemimicelles adsorbed at the HOPG/solution interface before and after solubilization of styrene are studied by AFM. Fig. 1b is an AFM image captured in situ on HOPG in the styrene and $C_{12}E_5$ ethanolic solution. It shows a nanostripe pattern that is similar to Fig. 1a, which is captured in 0.11 mM $C_{12}E_5$ aqueous solution. The nanostripes are less straight than those of pure $C_{12}E_5$. The nanostripe periodicity of pure $C_{12}E_5$ is 5.5 to 6.0 nm, within the range of its micellar diameter [3]. The periodicity in Fig. 1b, between 8 to 12 nm, is larger than that in Fig. 1a. This expansion is consistent with the styrene solubilization in the interior of the $C_{12}E_5$ hemimicelles. It is likely that the hemimicelle structure is perturbed by styrene solubilization, which also explains the less defined nanostructure in Fig. 1b.

The force-versus-distance curves captured in solution also show differences between the two cases. During the AFM force measurement, the interaction force between the AFM tip and the substrate is recorded as a function of their separation in solution. A repulsive force arises when the adsorbed surfactant film resists the advancement and penetration of the AFM tip, also called the steric repulsion. When the resistance limit is reached, the AFM tip suddenly snaps onto the substrate because of the force gradient exceeding the spring constant. This sudden movement is called the jump-in point. It has been suggested that the jump-in point reflects the surfactant molecules being pushed out of the contact zone in a collective lateral movement [16]. The force curve captured in pure $C_{12}E_5$ is in Fig. 1c and the force curve captured in the mixed solution is in Fig. 1d. The film thickness is estimated from the repulsion onset to be 5.9 nm in pure $C_{12}E_5$ and 10 nm in the mixed solution. This expansion is consistent with the solubilization of styrene in the $C_{12}E_5$ hemimicelles. The main difference is that the push-out of the film molecules is less abrupt when styrene is present. In the absence of styrene, there is a clearly defined jump-in point signified by the large gap in data collection. The maximum steric force barriers are comparable (0.8 vs. 0.9 nN). The lack of such jump-in event suggests non-uniform molecular adsorption strength/mechanism at the surface, which hinders the collective movement of molecules. This is consistent with the adsorption of both $C_{12}E_5$ and styrene at the HOPG surface. The presence of styrene next to the alkyl chains of $C_{12}E_5$ may disrupt the uniform epitaxial interaction with the HOPG lattice. It is also possible that styrene disrupts the micellar structure and allows small domains to move independently from each other.

The hemicylindrical hemimicelle structure is depicted in Fig. 1e. Fig. 1f shows the schematic structure of $C_{12}E_5$ hemimicelles solubilized by styrene monomers at the interface.

It is uncertain if the surfactant surface phase undergoes any changes (i.e., phase separation) at higher reaction temperature ($\sim$ 65 °C). From the polymer rods obtained after reaction, it can be concluded that the hemicylindrical shape of the surfactant hemimicelles acts as a template and geometric confinement during styrene polymerization.

The contact angle of water on HOPG is measured to be $75 \pm 3°$. The contact angle of water on the polymerized film is measured to be $82 \pm 3°$, which compares favorably with literature contact angle of 80° of water on polystyrene [17].

Chloroform is used to remove some film materials for examination after surface polymerization. The effluent chloroform solution is examined by FTIR in the attenuated total reflection (ATR) Mode (Magna IR-560, Nicolet). The IR spectrum (Fig. 2) displays the characteristic peaks of polystyrene at 1458, 1495 and 1600 cm^{-1} [20].

Fig. 3a is an AFM image of the film after 1-h polymerization time. The ill-defined rod-like nanostructure has an average length = 100–350 nm, width = 8–18 nm, and height = 2–5 nm as determined by sectional height analysis. The width is estimated by the peak-to-peak distance between two neighboring rods. The height is estimated by the z distance between the center of the peak and the flat background. Fig. 3b is a height profile along the white line in Fig. 3a. The polymer rods are wider than the surfactant hemimicelles.

After 3 h of polymerization time, rods become larger with length = 1 μm, width = 60–85 nm, and height = 0.5–1 nm as shown in Fig. 3c. The height values are likely underestimated (Fig. 3d) because the

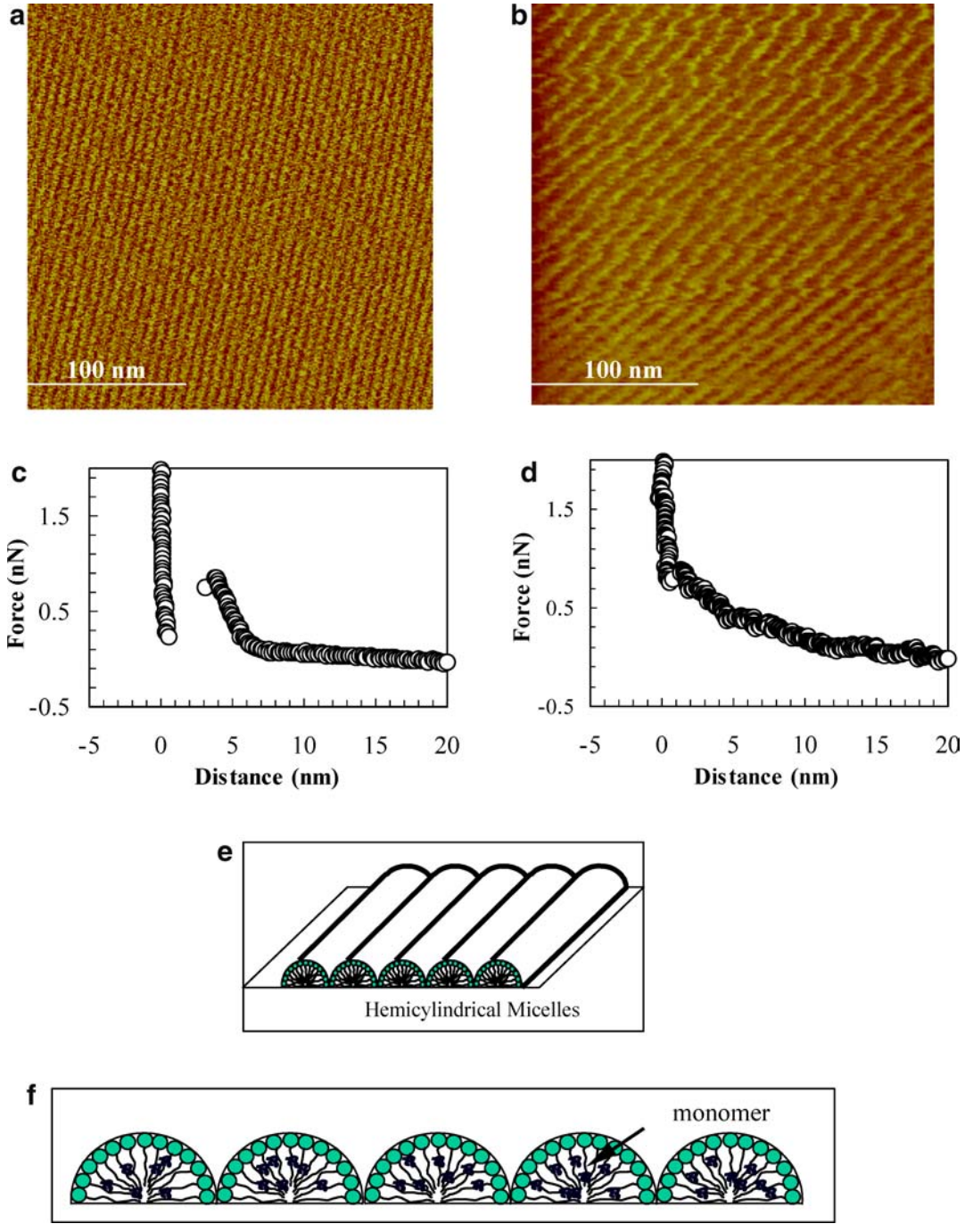

Fig. 1 $C_{12}E_5$ hemimicelles on graphite as a template for the synthesis of polystyrene. **a** AFM height image captured in the Contact Mode in 0.11 mM $C_{12}E_5$ solution on graphite. The nanostripes are hemicylindrical micelles epitaxially oriented on graphite. **b** AFM height image captured in the Contact Mode in 0.10 mM $C_{12}E_5$ and 0.05 M styrene mixed solution on graphite. **c** AFM force curve measured in 0.11 mM $C_{12}E_5$ solution on graphite. **d** AFM force curve measured in 0.10 mM $C_{12}E_5$ and 0.05 M styrene mixed solution on graphite. **e** Structure scheme of $C_{12}E_5$ hemicylindrical micelles on graphite. **(f)** Scheme of hemicylindrical micelles swollen by styrene monomers as viewed along the cross section of the surfactant hemicyliders

AFM tip cannot reach the HOPG when rods are close to each other and no flat background is present to serve as a baseline. Approximately 15% surface coverage consists of some flat and wide bands such as the one at the left lower corner in Fig. 3c. The width of the bands reaches approximately 350 nm. It indicates that polymerization is no longer confined by the initial geometry of the hemimicelles but proceeds in a lateral

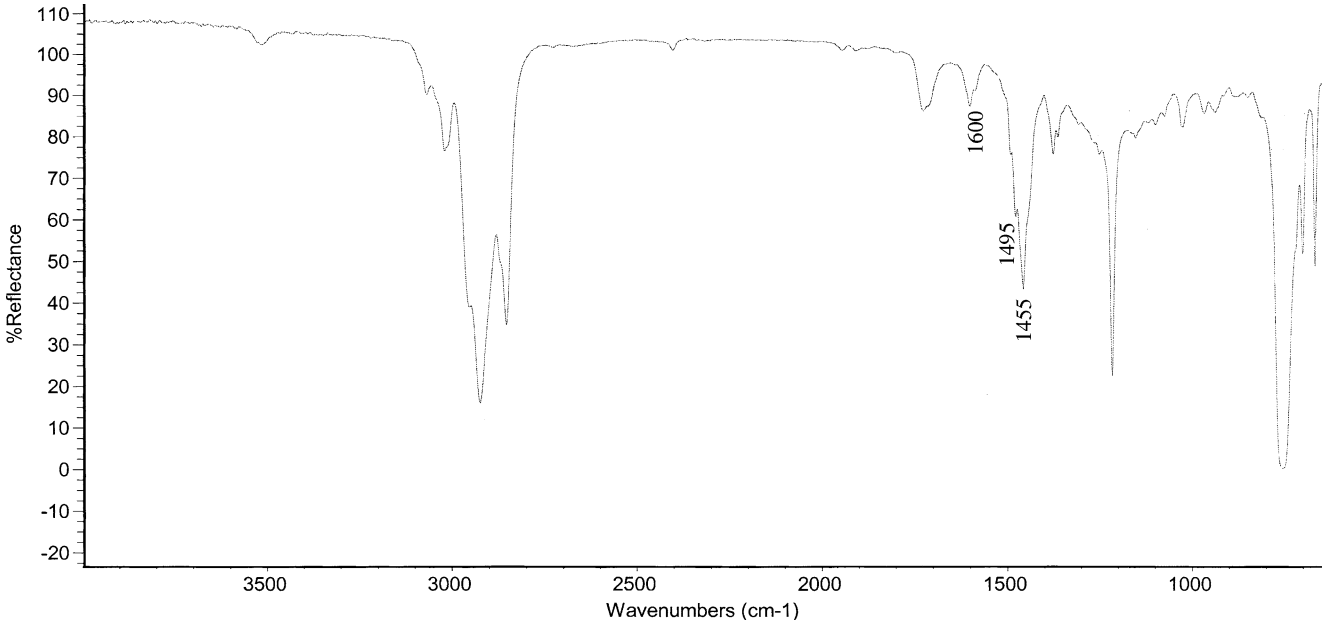

Fig. 2 IR spectrum of the film material removed from graphite by chloroform after polymerization

direction to form a 2-D structure. Another controlled experiment is also carried out with 3 h of reaction, but the monomer concentration is kept at a much higher value by not draining the solution from the surface before proceeding to polymerization. In that case, a thick continuous polystyrene film is formed.

Lateral growth of the polymer film has generally been observed in the admicelle polymerization [18]. A quasi-emulsion polymerization model has been postulated by Wu et al[18]. to describe the reaction behavior. The admicelles enriched in styrene on the surface act as both a reactor and the source of the monomer. The monomers dissolved in the bulk solution are non-negligible as compared to the emulsion polymerization, where monomers are only supplied by the emulsion droplets. Therefore, the transfer of monomers from supernatant fluids plays an important role in the surface polymerization to keep the polymer chain growing. If the chain growing direction is perpendicular to the long axis of the hemimicelles, the polymer cylinders will merge to form 2-D bands or eventually a continuous film. In our experiments, when the monomer solution is promptly removed from the surface, we observe the nanostructure growing with time and the nanorods merge with each other. But the continuous film is never observed probably because of monomer source deprivation. In the case when the monomer solution is left on the surface, the continuous and thick polystyrene film forms in a short time.

Polystyrene thin film formation on solid surfaces using admicelles polymerization has been extensively studied. Kitiyanan et al. [19] synthesized polystyrene films on precipitated silica using CTAB micelles in order to improve the function of silica as fillers in shoe soles and tires. Pongprayoon et al. [20] modified the cotton fiber surface with polystyrene to enhance water repellency and soil resistance. Polystyrene film was also successfully coated on glass fiber [21] and alumina [18]. This paper shows that the polymer chain aggregate morphology changes gradually with polymerization time. More detailed kinetic study with AFM is necessary to precisely control the size, shape, alignment, and distribution of polymer chains synthesized in the surfactant surface template down to the molecular level.

Conclusions

Parallel polystyrene nanorods are synthesized in the surfactant hemicylindrical hemimicelle template on HOPG. The film has been characterized in situ and ex situ by AFM, FTIR-ATR, and contact angle goniometry. The method shows a potential to vary the polymer nanorod width from 8 to 350 nm by controlling the reaction time and monomer concentration. The highly ordered polymer arrays have potential applications for surface modification and fabrication of nanopatterns for nanotechnological applications.

Experimental

The synthesis of polystyrene nanorods on graphite (HOPG ZYH grade, Advanced Ceramic Co.) uses the

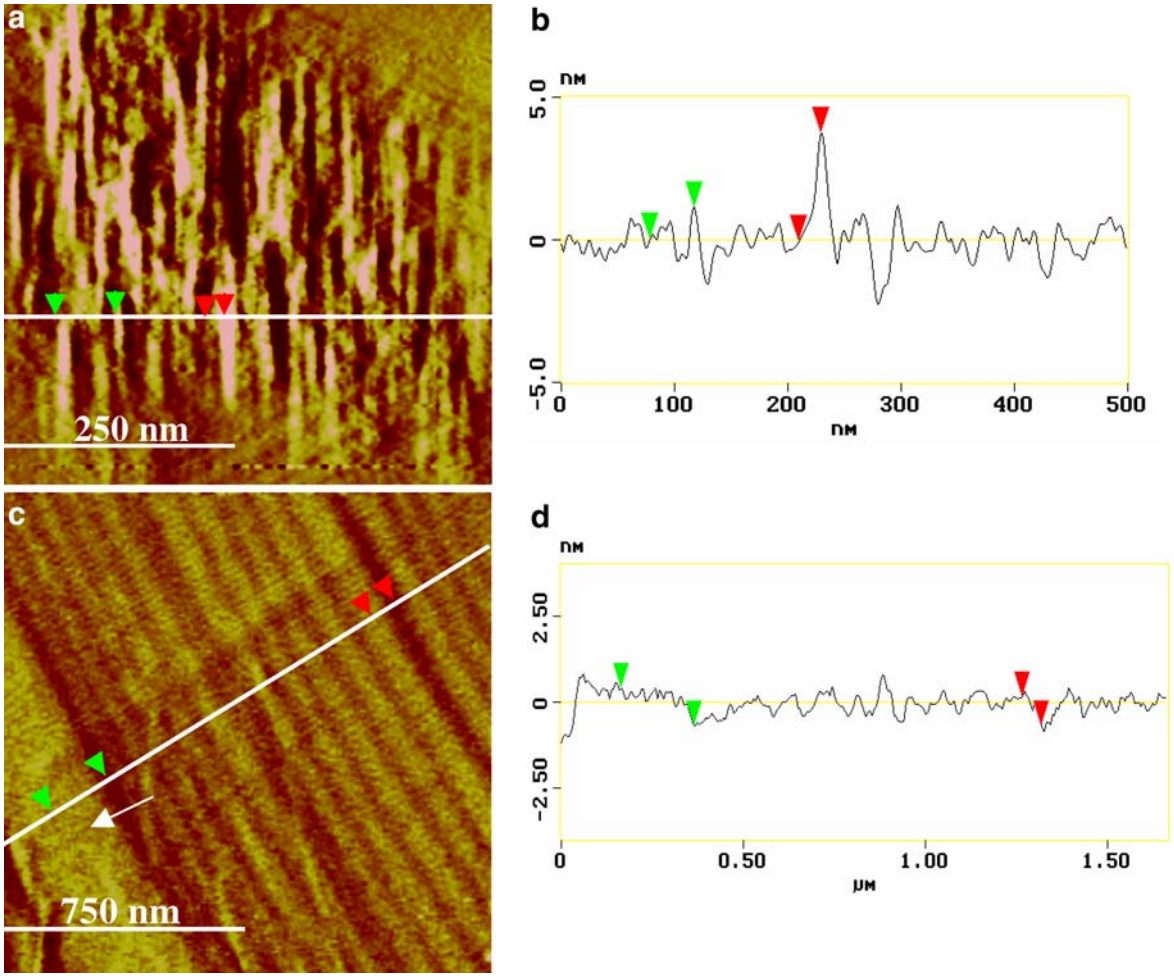

Fig. 3 AFM height images and height cross sectional profiles captured in the Contact Mode in air of polystyrene synthesized in $C_{12}E_5$ hemicylindrical hemimicelles on graphite. **a** Film after 1-h polymerization time, and **b** its cross sectional height profile along the *white line* in (**a**). **c** Film after 3-hour polymerization time, and **d** its corresponding cross sectional height profile along the *white line* in (**c**)

self-assembled template of nonionic penta(oxyethylene) dodecyl ether or $C_{12}E_5$ (98%, Fluka). $C_{12}E_5$ at 0.11 mM (= 2×CMC) forms the typical nanostripe pattern on HOPG due to the 1-D epitaxy between the zigzag alkyl chains and the HOPG carbon lattice.

The surface nanostructures are imaged by AFM (Digital Instrument, Nanoscope IIIa) in the Contact Mode using a fluid cell containing 0.11 mM $C_{12}E_5$ solution. An E-scanner with maximum scan area of 10×10 μm^2 is used. The z-scale of the scanner is calibrated with Ultra-Sharp Calibration *TGZ02* set (step height 100 nm, Silicon-MDT). Silicon nitride integral tips (NP type) are used with a nominal tip radius of 20–40 nm. In order to compare the force values, we present data that are obtained by the same cantilever tip. The spring constant of the cantilever is calibrated using the deflection method against a reference cantilever (Park Scientific Instruments) of known spring constant (0.157 N/m) [22]. The calibrated value 0.17 ± 0.05 N/m is used in all force plots. The force calibration curve is converted to the force-versus-separation plot following a standard procedure [23]. A representative force curve is selected from tens of curves measured on the same sample. A previous study has shown that the typical AFM force measurement errors in our system are ± 0.16 nN for the force magnitude and ± 0.5 nm for the separation distance [24]. The tip to substrate velocity is fixed at 0.2 μm/s in force calibration. We find that the force curves become independent of approach speed below 0.5 μm/s for the nonionic surfactant systems. The temperature is maintained at 22 ± 1 °C. AFM images of the surfactant layer are obtained in the soft-contact mode. The scan rate is between 3 and 12 Hz. Height images are captured with feedback gains between 3 and 5. Deflection images are captured with feedback gains less than 1. Height images are flattened in order to remove background slopes. No other filtering procedures are performed on these images.

The contact angle is measured by an NRL contact angle goniometer (Model 100, Rame-Hart) in the laboratory atmosphere. A water droplet of 20 μl is placed on the substrate and contact angles are read on both sides of the droplet. Five droplets are placed at various spots near the center of the substrate, and contact angles are averaged with an error of $\pm 3°$.

The procedures for surface polymerization are described as follows. 0.9 M styrene ethanolic solution is mixed with 0.11 mM $C_{12}E_5$ aqueous solution to form a saturated styrene solution. The styrene is added until it forms a saturated solution. The styrene concentration is approximately 0.05 M in the mixed solvent, while the $C_{12}E_5$ concentration is about 0.10 mM. The solutions were not degassed. After vigorous stirring of the mixture solution, a freshly cleaved graphite piece is immersed in the solution. The HOPG piece is kept in the solution for 2 h at room temperature. The solution is drained from the surface with only a thin liquid film remaining. The HOPG piece is then immersed in 0.05 M sodium persulfate (>99%, Aldrich) aqueous solution. The sodium persulfate concentration is kept the same as monomer according to literature [25]. The solution is heated to 65°C for 1 h during styrene polymerization. The surface is rinsed with deionized water and ethanol in order to remove surfactants and excess monomers. The contact angle of the surface no longer changes (~82°) after rinsing three times with water, each rinse lasting 10 s. The surface is dried with nitrogen gas before characterization.

Acknowledgments We acknowledge financial support from the National Science Foundation (CTS-0221586 and CTS-9703102) and Petroleum Research Fund (36149-AC5).

References

1. Davis HT (1996) Statistical mechanics of phases, interfaces, and thin films Chap. 6. VCH, New York
2. Manne S, Gaub HE (1995) Science 270:1480
3. Patrick HN, Warr GG, Manne S, Aksay IA (1997) Langmuir 13:4349
4. Lamont S, Reuben E, Ducker WA (1998) J Am Chem Soc 120:7602
5. Grant LM, Tiberg F, Ducker WA (1998) J Phys Chem B 102:4288
6. Tiberg F, Brinck J, Grant L (2000) Curr Opinion Colloid Interface Sci. 4:411
7. Dong J, Mao G, Hill RM (2003) AFM study of trisiloxane surfactant aggregate structures at the solid/liquid interface in mesoscale phenomena in fluid systems Chap 1. ACS Symposium Series 861, Washington DC
8. Bognolo G, Uniqema EB (2003) Adv. Colloid Interface Sci. 106:169
9. Beck JS, Vartuli JC, Kennedy GJ, Kresge CT, Roth WJ, Schramm SE (1994) Chem. Mater. 6:1816
10. Miller SA, Ding JH, Gin DL (1999) Curr Opin Colloid Interface Sci. 4:338
11. Clark Jr CG, Wooley KL (1999) Curr Opin Colloid Interface Sci. 4:122
12. O'Haver J, Grady B, Harwell JH, O'Rear EA (2001) Ad-micellar polymerization in surfactant science series, 100 reactions and synthesis in surfactant systems. Texter J (ed) Marcel Dekker, New York, pp. 537–545
13. Biggs S, Walker LM, Kline SR (2002) Nano Lett 2:1409
14. Carswell ADW, O'Rear ED, Grady BP (2003) Polymer Preprints 44:158
15. Carswell ADW, O'Rear ED, Grady BP (2003) J Am Chem Soc 125:14793
16. Ducker WA, Clarke DR (1994) Colloids Surf A 93:275
17. Tretinnikov ON, Stepanov BI (2000) Langmuir 16:2751
18. Wu J, Harwell JH, O'Rear EA (1987) J Phys Chem 91:623
19. Kitiyanan B, O'Haver JH, Harwell JH, Osuwan S (1996) Langmuir 9:2162
20. Pongprayoon T, Yanumet N, O'Rear EA (2002) J Colloid Interface Sci 249:227
21. Sakhalkar SS, Hirt DE (1995) Langmuir 11:3369
22. Tortonese M, Kirk M (1997) SPIE 3009:53
23. Dong J, Mao G (2000) Langmuir 16:6641
24. Wang A, Jiang L, Mao G, Liu Y (2001) J Colloid Interface Sci 242:337
25. Funkhouser GP, Arevalo MP, Glatzhofer DT, O'Rear EA (1995) Langmuir 11:1443